Cover Page

The handle http://hdl.handle.net/1887/139043 holds various files of this Leiden University dissertation.

Author: Boer, D.E.C.
Title: Glucocerebrosidase and glycolipids: In and beyond the lysosome
Issue Date: 2021-01-07

Chapter 3

In situ visualization of glucocerebrosidase in human skin tissue: zymography versus activity-based probe labeling

In situ visualization of glucocerebrosidase in human skin tissue: zymography versus activity-based probe labeling

J. van Smeden, I.M. Dijkhoff , R.W.J. Helder, H. Al-Khakany, **D.E.C. Boer**, A. Schreuder, W.W. Kallemeijn, S. Absalah, H.S. Overkleeft, J.M.F.G. Aerts, J.A. Bouwstra.

Abstract

Epidermal β-glucocerebrosidase (GCase), an acid β-glucosidase normally located in lysosomes, converts (glucosyl)ceramides into ceramides, which is crucial to generate an optimal barrier function of the outermost skin layer, the stratum corneum (SC). Here we report on two developed *in situ* methods to localize active GCase in human epidermis: i) an optimized zymography method that is less labor intensive and visualizes enzymatic activity with higher resolution than currently reported methods using either substrate 4-methylumbelliferyl-β-D-glucopyranoside or resorufin-β-D-glucopyranoside; and ii) a novel technique to visualize active GCase molecules by their specific labeling with a fluorescent activity-based probe (ABP), MDW941. The latter method pro¬ved to be more robust and sensitive, provided higher resolution microscopic images, and was less prone to sample preparation effects. Moreover, in contrast to the zymography substrates that react with various β-glucosidases, MDW941 specifically labeled GCase. We demonstrate that active GCase in the epidermis is primarily located in the extracellular lipid matrix at the interface of the viable epidermis and the lower layers of the SC. With ABP-labeling, we observed reduced GCase activity in 3D-cultured skin models when supplemented with the reversible inhibitor, isofagomine, irrespective of GCase expression. This inhibition affected the SC ceramide composition: MS analysis revealed an inhibitor-dependent increase in the glucosylceramide:ceramide ratio.

Introduction

Epidermal β-glucocerebrosidase (GCase), an acid β-glucosidase normally located in lysosomes, converts (glucosyl)ceramides into ceramides, which is crucial to generate an optimal barrier function of the outermost skin layer,

the stratum corneum (SC). Here we report on two developed *in situ* methods to localize active GCase in human epidermis: *i*) an optimized zymography method that is less labor intensive and visualizes enzymatic activity with higher resolution than currently reported methods using either substrate 4-methylumbelliferyl-β-D-glucopyranoside or resorufin-β-D-glucopyranoside; and *ii*) a novel technique to visualize active GCase molecules by their specific labeling with a fluorescent activity-based probe (ABP), MDW941. The latter method pro¬ved to be more robust and sensitive, provided higher resolution microscopic images, and was less prone to sample preparation effects. Moreover, in contrast to the zymography substrates that react with various β-glucosidases, MDW941 specifically labeled GCase. We demonstrate that active GCase in the epidermis is primarily located in the extracellular lipid matrix at the interface of the viable epidermis and the lower layers of the SC. With ABP-labeling, we observed reduced GCase activity in 3D-cultured skin models when supplemented with the reversible inhibitor, isofagomine, irrespective of GCase expression. This inhibition affected the SC ceramide composition: MS analysis revealed an inhibitor-dependent increase in the glucosylceramide:ceramide ratio.

β-Glucocerebrosidase (GCase; also referred to as acid β-glucosidase or GBA; EC 3.2.1.45) is a lysosomal enzyme that hydrolyzes glucosylceramides (GlcCers) into ceramides [1, 2]. Inherited GCase deficiency (as occurs in Gaucher disease) results in lysosomal accumulation of GlcCers, primarily in macrophages located in the liver, spleen, and bone marrow [3]. Complete absence of GCase causes an extreme Gaucher disease phenotype (so-called collodion baby) with fatal skin abnormalities [4]. Newly synthesized GCase is normally transported to

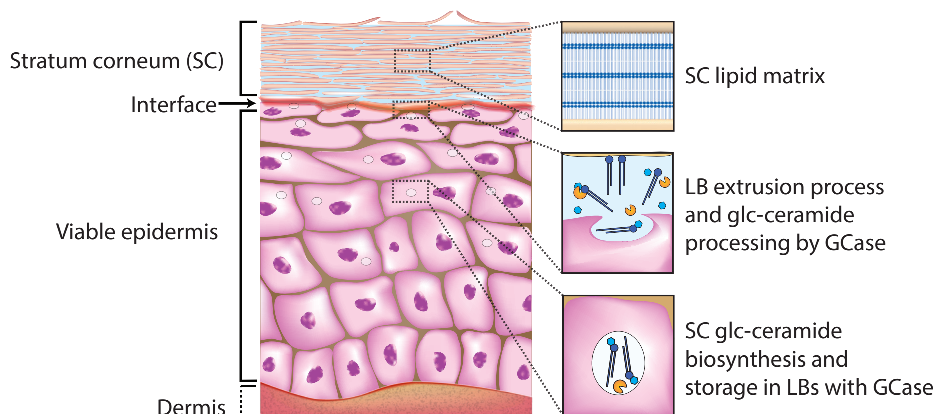

Figure 1: Epidermis with the outermost layer (SC) functioning as the primary skin barrier. The biosynthesis of the SC ceramides is located in the lower and middle epidermal layers, while storage takes place at the lamellar bodies together with processing enzymes like GCase. Once extruded at the interface of the viable epidermis and the SC, GCase converts the GlcCers into their final barrier components, the ceramides, which become part of the ordered SC lipid matrix.

the lysosomal compartment by binding to the lysosomal integral membrane protein type-2 [5]. In lysosomes, GCase is active at its optimal pH of around 5.2–5.6, assisted by the activator protein, saposin C [6, 7]. Besides lysosomal GCase, two other β-glucosidases can be present in cells (GBA2 and GBA3). GBA2 can also convert GlcCers into ceramides, implicating that such conversion may also occur outside the lysosomes [8]. Here, GCase is used when specifically referring to lysosomal β-glucosidase, whereas any β-glucosidase is indicated as GBA.

To date, over 270 *GBA* mutations have been identified (https://research.cchmc.org/LOVD2/) that may either lead to reduced protein expression or result in nonfunctional GCase or a reduced enzyme activity [9]. GCase expression levels do not often relate to enzyme activity because of various aspects, like posttranslational modifications of the protein or cofactors [10]. This suggests that GCase activity (rather than gene or protein expression) is indicative for the clinical outcome. However, current studies on lipid metabolic enzymes mainly focus on methods to quantify gene expression or protein levels, rather than enzyme activity. To date, enzyme activity is often performed via zymography studies in which a selective substrate is converted to a fluorescent product by the enzyme of interest. Many *in vitro* and *in situ* methods have been established, particularly for studies on proteases [11-13]. Reports on zymography of other enzymes are less common, but GCase is an excellent example in which established methods have proven their value: 4-methylumbelliferyl-β-D-glucopyranoside (4-MU-β-glc) has been used as a substrate and is converted by GCase into the blue fluorophore, 4-methylumbelliferone ($\lambda_{em,max} \approx$ 450 nm; supplemental Figure S1) [7]. A common alternative is resorufin-β-D-glucopyranoside (res-β-glc), which results in red fluorescent resorufin ($\lambda_{em,max} \approx$ 580 nm). The substrates are limited in their sensitivity and substrate specificity is a matter of concern. Alternatives to zymography are therefore needed to examine the presence of active GCase, like the use of activity-based probes (ABPs) [14, 15]. This technique relies on mechanism-based labeling of GCase with a fluorescent suicide inhibitor [16, 17]. MDW941 is a cyclophellitol β-epoxide tagged with a BODIPY red dye (supplemental Figure S1) [16]. It binds covalently to the catalytic nucleophile, E340, of GCase with high affinity and specificity. Fluorescent ABPs like MDW941 have been successfully used to visualize *in situ* active GCase molecules in cultured cells and tissues of rodents [16, 18], but human skin tissue has so far never been examined with these ABPs.

The aim of this study was to develop, optimize, and compare zymography and ABP-labeling to visualize *in situ* active GCase in human skin tissue. Human skin contains a dermal and an epidermal component, the latter consisting of several layers, including the stratum corneum (SC), the nonviable outermost skin layer (Figure 1). This layer acts as a pivotal barrier and contains terminally differentiated enucleated cells embedded in a ceramide-rich lipid matrix [19]. In this matrix, ceramides are a major component and have uniquely long

hydrocarbon chains [20]. Changes in the composition of SC ceramides or the expression of GCase may lead to an impaired barrier function that has been encountered in several inflammatory skin diseases (e.g., eczema) [21, 22]. These ceramides are synthesized in the endoplasmic reticulum of viable epidermal cells [23-25] and are subsequently stored as GlcCers in vesicles (so-called lamellar bodies) together with GCase and other enzymes that convert the lipid precursors into barrier lipids [26]. This conversion occurs during the lamellar body extrusion process: the lamellar bodies fuse with the cell membrane and extrude their lipid and enzyme content into the extracellular space between the viable epidermis and the SC [20]. To date, it has been reported that the conversion of GlcCers into ceramides by GCase takes place in this lipid-rich environment [27, 28]. Subsequently, the ceramides are arranged into lipid layers (together with other barrier lipids, like fatty acids and cholesterol) forming

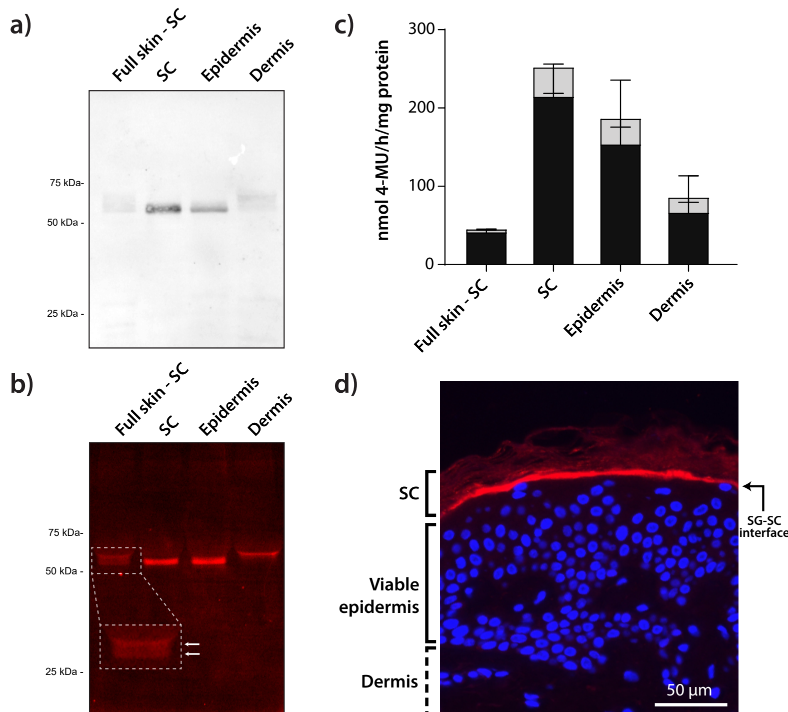

Figure 2: Labeling of GCase in human skin tissue. A: Western blot of GCase in different human skin tissue layers using monoclonal anti-GCase (50 mg of protein per lane were loaded on the SDS-PAGE gel). Full skinSC, full thickness skin without SC. B: Fluorescent labeling of active GCase (5 mg of protein per lane were loaded on the SDS-PAGE gel) in skin tissues exposed to MDW941. C: Bar plots of the enzymatic activity of GCase in skin tissue, as determined by a 4-MU-b-glc substrate assay (gray + black bars). The fraction of 4-methylumbelliferone converted by GCase is indicated by black bars (n = 3, mean ± SD). D: Immunohistochemical fluorescent staining of expressed GCase (red), and counterstaining with DAPI (blue) for cell nuclei. Objective lens magnification 20×.

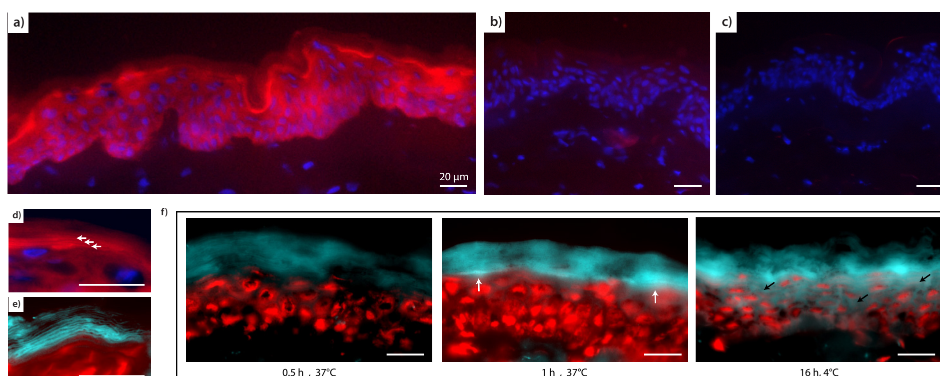

Figure 3: GCase *in situ* zymography assay on human skin sections. A: Microscopy photographs of 20× magnification using res-β-glc substrate (red) and DAPI counterstaining to detect cell nuclei (blue). B: Additional preincubation with competitive GCase inhibitor, resorufin, successfully obstructs substrate conversion. C: No red fluorescence is observed when no substrate is applied (negative control). D: Photograph (63× magnification) in which the red fluorescent product layers are indicated by the white arrows. E: Images (63× magnification) using 4-MU--β-glc substrate focusing on the blue fluorescent product layers. Red counterstaining was performed using propidium iodide to stain cell nuclei. F: Microscopy images (63× magnification) of the results from different substrate incubation periods (0, 1, and 16 h). White arrows indicate highest signal contrast, whereas black arrows illustrate the diffusion effect of the fluorescent product at longer time periods. Scale bars represent 20 mm.

lamellar stacks. These lamellar stacks function as the principal barrier and are crucial to protect the body from the environment [29, 30]. The conversion of GlcCers into ceramides by GCase in the extracellular space is contradictory to the notion that GCase is solely active in the lysosomal compartment [2, 31]. Using two newly developed techniques (zymography and ABP-labeling), we were able to visualize active β-glucosidase and, more specifically, active GCase.

First, the presence of GCase from isolated skin layers was demonstrated and the specificity of the ABP for GCase (MDW941) in skin lysate was determined. Second, an optimized *in situ* zymography method was developed, as current methods for visualizing GCase activity in skin sections have substantial (conflicting) differences in their procedures [7, 32, 33]. Third, a new method to detect GCase in human epidermis by means of *in situ* ABP-labeling was optimized in regard to ABP concentration, buffer conditions, and washing procedures. This method was applied on a cultured 3D-human skin equivalent (HSE) model that mimics human skin [34], while the culture medium was supplemented with the GCase inhibitor, isofagomine (supplemental Figure S1). Isofagomine selectively inhibits GCase at low nanomolar concentration, but not the other β-glucosidases, GBA2 and GBA3 [35, 36]. This enabled us to study whether inhibition of GCase activity directly affects the SC glucosyl (ceramide) composition.

Results

GCase is primarily located near the interface of the viable epidermis and the SC.

IsIsolated lysates of human dermis, epidermis, SC, and the viable skin layers minus the SC (full skin-SC) were analyzed by Western blotting for the presence of GCase protein. GCase (~60 kDa) was expressed more in the epidermis than the dermis (Figure 2A). More specifically, GCase was predominantly located in the SC, as the viable skin layers (skin without SC) showed protein bands with much lower intensity. In addition to the Western blot procedure, we used the ABP, MDW941, to fluorescently label active GCase in skin tissue (Figure 2B; fluorescent bands at ~60 kDa; Coomassie brilliant blue staining for total protein content is provided in supplemental Figure S2). Interestingly, GCase located in the dermis appears to have a slightly higher molecular mass compared with GCase in the epidermis, which matches the presence of two bands in the lysate with epidermis and dermis (full-thickness skin minus SC). Subsequently, a 4-MU-β-glc activity assay was performed to quantify the activity of GCase in the different skin layers (Figure 2C). In all skin layers, GCase was shown to be primarily GCase and had the highest activity in epidermal tissue and SC tissue. This is in line with the Western blot and gel electrophoresis results presented in Figure 2A, B, where the most pronounced bands were observed in the epidermis and SC as well. We then performed *in situ* immunohistochemical staining to determine the exact location of GCase expression (Figure 2D). In line with the aforementioned results, GCase proved to be expressed in the viable epidermis and SC layers, predominantly along the whole interface of the viable epidermis and the SC. Having confirmed that GCase was predominantly expressed and active in epidermal skin layers and amenable to selective labeling by MDW941, we next established detailed protocols for localizing active GCase in human skin tissue. We focused on two *in situ* techniques: i) zymography of GCase, and ii) ABP-labeling of GCase.

In situ *zymography of epidermal GCase: method development of 4-MU-β-glc and res-β-glc substrates.*

We optimized the zymography protocol for two commonly used substrates, 4-MU-β-glc and res-β-glc, which, upon conversion by GCase, lead to their fluorescent products, 4-methylumbelliferone (indigo) and resorufin (orange/red). The procedure to obtain the high resolution *in situ* zymography images was an important aspect of the optimization procedure. We optimized the protocol for the following four important aspects concerning substrate reconstitution, washing procedure, substrate incubation buffer, and incubation period and temperature. First, res-β-glc is relatively insoluble in buffer solution, leading to fluorescent clusters that interfere with imaging. Dissolving the substrate in dimethylsulfoxide (i.e., 1 mM) prior to dilution in

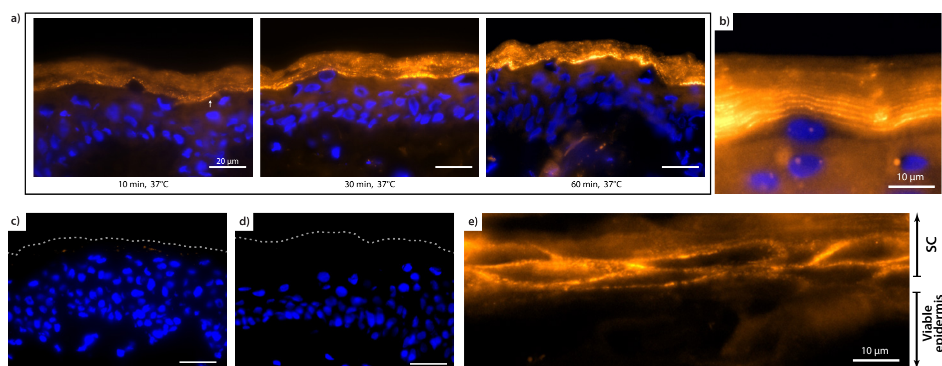

Figure 4: *In situ* GCase labeling by MDW941 ABP. Microscope images (63× magnification) of human skin sections incubated with the ABP, MDW941 (yellow/orange), and counterstained with DAPI (blue). Scale bar represents 20 mm unless stated otherwise. A: Incubation period assay of 10, 30, and 60 min incubation periods. At 10 min, some weak ABP-labeling is already present (white arrow). B: When zooming in on the viable epidermis-SC interface, prominent labeling of active GCase is observed. C: Competition assay of ABPs in which human skin sections were preincubated with nonfluorescent ABP (cylophellitol-epoxide tagged with a nonfluorescent moiety) prior to incubation with MDW941. The dotted line indicates the outermost SC layer. D: Human skin sections incubated without any ABP (negative control). E: High magnification of the viable epidermis-SC interface at skin sections in which the SC was not flattened, illustrating MDW941 labeling around the corneocytes (DAPI-counterstaining of nuclei in the viable epidermis is not visualized for better visualization of GCase in the extracellular lipid matrix).

buffer completely removed this. The 4-MU-β-glc could be dissolved directly in buffer, without any additional steps. Second, after incubation with substrate, washing is necessary to successfully remove background staining. Three short rinses with MilliQ water (the first one in addition with Tween-20) resulted in the best contrast between fluorescent signal and aspecific staining. Longer or more wash steps resulted in significant loss of fluorescent signal, whereas less washing led to reduced contrast. Third, we incubated the samples with two commonly used substrate buffers for zymography, 10 mM MES solution and 150 mM McIlvaine solution. Fourth, the effect of incubation period and temperature was investigated, using an incubation period between 0 and 16 h at 4°C or 37°C.

The results on the optimized protocol are depicted in Figure 3 (and supplemental Figure S3). Both substrates visualized GCase in skin sections and provided similar results: fluorescent product was observed at the viable epidermis-SC interface of human skin sections (Figure 3A). To exclude nonspecific staining, we performed a competition assay in which we preincubated skin sections with a commonly used competitive GCase-specific inhibitor, isofagomine. Consecutive incubation with substrate res-β-glc (in addition to equimolar concentrations of isofagomine to maintain

competition) resulted in no significant staining (Figure 3B), indicating that isofagomine successfully inhibited GCase activity and that the substrates were indeed converted by GCase. Without any substrate (negative control), no staining was observed either (Figure 3C). When studying the catalytic conversion of substrate by GCase at higher magnification levels (e.g., 63×), "layers" of fluorescent product were formed, as can be seen from Figure 3D and the zoomed section. The presence of GCase activity in the intercellular SC regions was also clearly visualized when using 4-MU-β-glc as substrate (Figure 3E). Incubation for at least 1 h at 37°C did result in sufficient fluorescent signal at the viable epidermis-SC interface. It was determined that longer incubation periods (e.g., 16 h) should be avoided to prevent excessive diffusion of fluorescent product throughout the section, even at the reduced temperature of 4°C (Figure 3F).

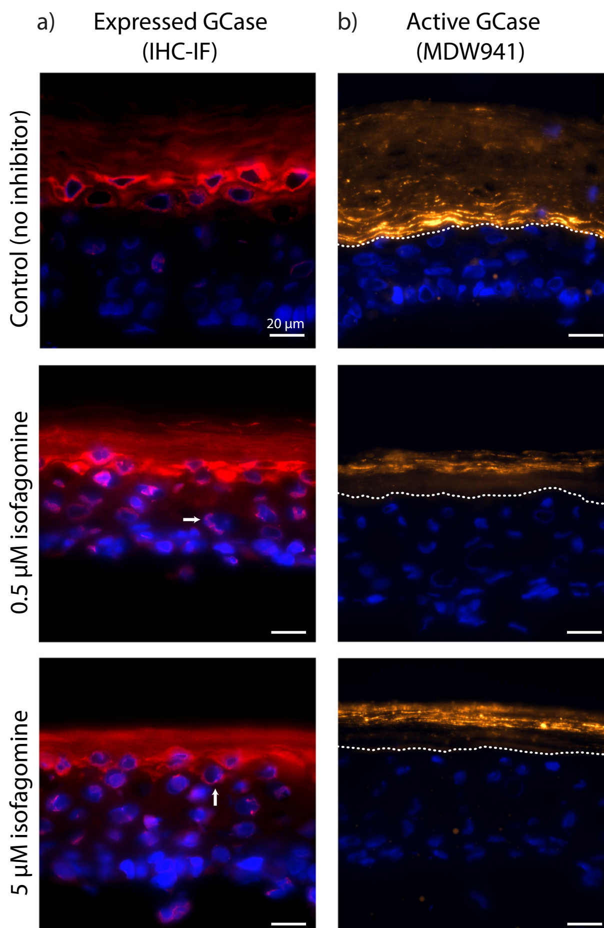

Figure 5: A: Immunohistochemical fluorescent staining of expressed GCase (red) in HSEs cultured with isofagomine or without (control). DAPI was used for counterstaining, indicating blue-labeled cell nuclei. White arrows point to GCase labeling near the nuclei of viable keratinocytes. B: In situ visualization of active GCase labeled with MDW941 in HSEs cultured with isofagomine. Yellow/orange staining (MDW941) indicates active GCase. Blue indicates cell nuclei (DAPI). All images were taken at a 63× magnification. Scale bar represents 20 µm. The dotted line indicates the viable epidermis-SC interface.

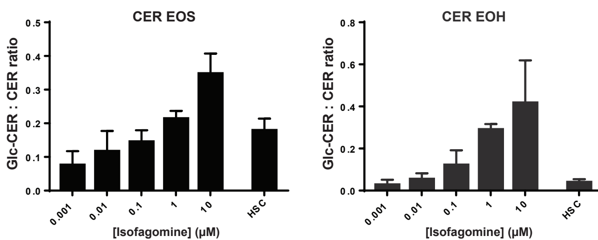

Figure 6: GlcCer:ceramide ratios of ceramide (CER) subclasses EOS and EOH in HSEs cultured with different concentrations isofagomine. Bar plots depict mean ± SD from three independent donor experiments with at least two or more cultures per experiment. As a control, a pool of >10 human SC samples was analyzed (HSC condition).

Developing an in situ *ABP-labeling procedure for localizing active GCase in the epidermis.*

We established a new method for visualizing active GCase in human epidermal skin tissue by means of ABP-labeling. We optimized the method for ABP concentration, incubation period, buffer type, and washing procedure. Concerning ABP concentration, labeling was already successful at 10 nM MDW941; however, more robust and high contrast staining was obtained at 100 nM concentrations. Higher concentrations (e.g., 1 µM) did not result in more intense staining, but increased the risk of nonspecific labeling (precipitation of the probe) (see supplemental Figure S4). When optimizing incubation period, we demonstrated that labeling was already observable after 30 min of incubation, but an ~1 h incubation period proved optimal (Figure 4A). At 63× objective lens magnification, it became apparent that GCase was present not only at the viable epidermis-SC interface but also in the lower SC layers, as fluorescent layers of ABP-labeling appeared (Figure 4B), similar to the fluorescent layers observed with the zymography method. To exclude that MDW941 labels at nonspecific sites of the skin sections, we preincubated sections in excess of a nonfluorescent selective GCase probe [37, 38]. This nonfluorescent probe binds covalently to E340 of GCase only. Its irreversible binding prohibits binding of MDW941 in the subsequent incubation period. Indeed, Figure 4C demonstrated no visible fluorescent signal (thus no MDW941 binding), illustrating specific labeling of active GCase by MDW941 in human skin sections. No background staining was observed, as incubation without ABP (negative control samples) resulted in no detectable staining (Figure 4D). MDW941 labeling on skin that was not fully differentiated (and thus shows no full flattening of the corneocytes in the SC) revealed that the ABP was located in the lipid matrix surrounding the corneocytes (Figure 4E). Note that when optimizing buffer, we obtained identical results when using MES and McIlvaine buffer; therefore, both buffers are considered suitable for ABP-labeling. Regarding washing procedure, we observed that washing at least three times proved superior over washing once, as the latter procedure did not always remove all unlabeled MDW941. The newly developed GCase

ABP-labeling proved quick and very reproducible, resulting in high resolution imaging, even at low concentrations of MDW941. This method was therefore used to study GCase expression in HSEs in which GCase activity was modulated.

Altered GCase activity in HSEs cultured with isofagomine.

We applied our optimized *in situ* ABP method to a HSE that resembles, to a large extent, the morphology and lipid composition in human skin. During generation of these HSEs, the medium was supplemented with 0–100 µM isofagomine, a potent reversible GCase inhibitor. We analyzed to what extent GCase expression and activity were affected by isofagomine in culture medium. Figure 5A shows that GCase in HSEs (as visualized with a specific antibody) was mainly located at the viable epidermis-SC interface, similar to the observations made for human skin (Figure 2D). This expression at the viable epidermis-SC interface was not decreased when cultured with 0.5 or 5 µM isofagomine in the medium. In fact, GCase expression was observed throughout all SC layers. Besides, adding isofagomine to the culture medium resulted in more GCase staining near the nuclei of viable epidermal cells (see arrows in Figure 5A), which implied an increase in *de novo* GCase expression and thus GCase synthesis. When analyzing the presence of active GCase using the ABP, MDW941, in the absence of isofagomine, labeling was observed at the viable epidermis-SC interface and the lower SC layers (Figure 5B), in line with the expression pattern observed in Figure 5A. Interestingly, labeling of active GCase at the viable epidermis-SC interface was lost when inhibitor (0.5 and 5 µM) isofagomine was added to the medium. Only a weak staining at the outermost SC layers remained.

SC ceramides in HSEs are altered when cultured with isofagomine.

Because we observed changes in GCase in HSEs cultured with the inhibitor, isofagomine, we analyzed the SC ceramides of these HSEs by means of LC/MS. Figure 6 depicts the GlcCer:ceramide ratios of two acylceramide subclasses, EOS and EOH, respectively. At 1 nM isofagomine concentration (far below the Ki,isofagomine of ~20 nM) [39], a ratio around 0.8 was observed, indicating that ~7% of ceramide EOS remained glycosylated at this culturing condition. When the isofagomine concentration was increased, the GlcCer:ceramide ratio was also increased for both ceramide EOS and EOH. At concentrations of 10 µM isofagomine, the ratio increased significantly to 0.35 ± 0.06 and 0.42 ± 0.20 for EOS and EOH, respectively. This indicated that the conversion of GlcCers into ceramides was successfully hampered by the competitive inhibitor, isofagomine. The HSE model can therefore be supplemented with specific concentrations to modulate the exact amount of GlcCers:ceramides.

Discussion

This study first reported on the presence of active GCase in human skin, which was primarily located outside the lysosomes in the extracellular space of the inner layers of the lipophilic SC lipid matrix. GCase activity in such an environment is unique and has hitherto not been observed in any other tissues. We described two independent methods to visualize the presence of active GCase in the extracellular space: zymography and ABP-labeling. Although the presence of GCase at the viable epidermis-SC interface has been reported before using zymography [7, 32, 33, 40-42], the specificity of the substrates (res-β-glc and 4-MU-β-glc) has been debated, as both are converted by several β-glucosidases [43-45]. Therefore, we developed a new method that uses the ABP, MDW941. This aziridine-based probe has unmatched sensitivity and specificity toward lysosomal GCase and delivers superior spatial resolution images. Below, we discuss and compare both methods (summarized in Table 1).

Zymography.

The developed procedure is compatible with the two most commonly used substrates in relation to GCase activity. The method is robust, less time-consuming, and provides higher resolution images than most reported protocols. The following optimization steps proved crucial for the improved results, and are related to sample preparation, incubation period, choice of substrate, incubation buffer, and washing procedures.

First, reported *in situ* methods sometimes use fixation solvents to localize GCase activity [7, 32], but this mitigates GCase activity and should be avoided [46-48]. Cryo-fixed sections without fixation solvent on SuperFrost glass slides are therefore preferred.

Second, the optimal incubation period with 4-MU-β-glc or res-β-glc was around 1–2 h. Shorter incubation periods led to significantly less fluorescent product, whereas longer incubation periods caused diffusion of the fluorescent product. Takagi et al. [7] proposed an incubation period of 16 h at the reduced temperature of 4°C to minimize diffusion of product, but our proposed method demonstrated clearer contrast of converted product when applying an incubation period of less than 2 h at 37°C. Besides, incubation at 37°C more closely resembles the *in vivo* situation and, thus, the physiological activity of GCase.

Third, no significant difference was observed between the two substrates, res-β-glc (orange/red) and 4-MU-β-glc (indigo), for *in situ* visualization of active GCase. Neither substrate showed significant overlap in its emission wavelength with its respective counterstain (DAPI and propidium iodide). Green fluorophores were avoided because of the autofluorescence of skin tissue caused by components like collagen, elastin, melanin, and keratin [49,

50]. We did not observe any emitted fluorescence signal for res-β-glc at the excitation and emission wavelengths proposed by Hachem et al. [33] (588 and 644 nm, respectively).

Fourth, GCase activity is optimal around pH 5.2–5.6 [6, 7]. The use of appropriate buffers is therefore crucial and preferred over the use of deionized water as the substrate solvent, as has been used in other protocols [33]. MES buffer (10 mM) was preferred over 150 mM McIlvaine buffer, as the images were more consistent and more often resulted in clear "layered" patterns of converted fluorescent product in the SC. This could be related to the high salt concentration of McIlvaine buffer, which may affect the surface charge and tertiary structure of GCase, leading to changes in enzyme activity [51].

Fifth, we noticed significantly better results after optimizing the washing steps. Directly after cryo-sectioning, protocols should include a washing procedure to remove specimen matrix (e.g., Tissue-Tek). In agreement with Man et al. [52], we observed that the matrix was easily removed when washing with 1% Tween-20 in water. A second washing step was introduced directly after the substrate incubation step. A dip-wash with deionized water that was repeated three times appeared to be optimal; the first wash was with the addition of 1% Tween-20.

ABP-labeling.

ABP-lABP-labeling has several advantages compared with the zymography procedure: *i*) MDW941 labeling proved much more sensitive, as incubation with 100 nM ABP was sufficient for proper localization, whereas 1 mM substrate was preferred for zymography. *ii*) MDW941 is GCase specific, in contrast to 4-MU-β-glc and res-β-glc, which are ligands for all β-glucosidase subtypes (GCase, GBA2–3). Hence, only the ABP-labeling method demonstrated that visualized protein is indeed lysosomal GCase. *iii*) Covalent binding of ABP was less dependent on incubation period and washing procedures, and labeling with the ABP, MDW941, does not require enzyme-based protonation (thus incubation near optimal pH) [37]. *iv*) Generally, reproducibility of *in situ* zymography is a main concern and repeated measurements are necessary to compensate for irregular results [53]. In contrast, ABP-labeling delivers more robust images of active GCase along the entire skin section. As a consequence, ABP-labeling requires a significantly lower number of skin sections for reliable conclusions in comparison to zymography.

Recapitulating, this is the first time that the highly sensitive and selective MDW941 label demonstrates that active GCase is located in the lipophilic extracellular matrix outside the lysosomes of human skin, which is unique with respect to both environmental condition and localization as observed in cells of other tissues [16, 18]. ABP sensitivity also becomes apparent when comparing ABP-labeling to the *in vitro* Western blotting procedure:

for successful visualization of GCase, only 5 µg of protein was loaded for the ABP-labeling procedure, whereas 50 µg was required for the Western blot procedure. ABP-labeling of skin lysates demonstrated that active GCase in the dermis is of different molecular size than active GCase in the epidermis. This suggests that different isoforms are present in both skin layers, consistent with our finding that N-glycanase treatment converted both dermal and epidermal GCase to an identical molecular weight [54-56]. In the dermis, GCase is likely located in the lysosomes of cells (fibroblasts, macrophages, and adipocytes), where it degrades GlcCer as the penultimate step in cellular glycosphingolipid turnover.

The unmatched sensitivity of ABP-labeling proved useful when studying HSEs. GCase expression and activity in HSEs is localized at the same epidermal layers compared with human skin. Supplementation of isofagomine, a commonly used potent reversible inhibitor of GCase [45, 57, 58], to the medium demonstrated that the activity of GCase can be altered without significantly reducing GCase expression or inducing any morphological effects. Localization of active GCase in the epidermis is therefore essential for understanding the consequences of the SC ceramide composition. Inhibition of GCase by isofagomine resulted in a concentration-dependent increase of the precursors, acyl-GlcCer EOS and acyl-GlcCer EOH, compared with their acyl-ceramide products. We specifically studied these two ceramide subclasses, as it is known that ceramides EOS and EOH are not substrates for a second enzyme (acid sphingomyelinase) that converts sphingomyelins into ceramides [59]. A high concentration of isofagomine in the medium led to complete inhibition of GCase at the viable epidermis-SC interface and only a weak ABP-labeling in the outer SC layers was observed. This indicates that isofagomine reaches the SC layers and proves that GCase activity is crucial for the SC ceramide composition. We explain GCase activity in the outer SC layers by the fact that isofagomine may not sufficiently diffuse into the upper SC layers and inhibit GCase. Besides, competition between substrates, endogenous GCase, and isofagomine still occurs, as isofagomine is a reversible inhibitor and the medium is refreshed twice a week. Any remaining GCase activity is therefore expected to be at the lowest isofagomine concentration, i.e., the outermost SC layers. Nevertheless, the concentration-dependent effect indicates that the conversion by GCase can be modulated by hampering enzyme activity, irrespective of GCase expression. This supplement may therefore be useful to target GCase to model skin barrier dysfunction related to specific diseases. Gaucher disease is an obvious candidate, but a dysfunction in GCase expression is also observed in skin disorders like Netherton syndrome and atopic dermatitis [21, 60]. The significance of GCase activity in these skin diseases remains inconclusive [61, 63] and the presented methods here will be used in future studies to unravel this aspect, along with the relationship to environmental factors, like skin

Table 1: Overview of the optimized *in situ* protocols to visualize epidermal GCase by zymography and ABP-labeling.

Parameter	*In situ* Zymography	*In situ* ABP-Labeling
Section fixation	Cryo-samples (no fixation)	Cryo-samples (no fixation)
[Fluorogenic compound]	~1 mM 4-MU-b-glc or res-b-glc	~100 nM MDW941
Incubation period/temperature	1–2 h, 37°C	1 h, 37°C
Preferred buffer	MES	MES or McIlvaine
Washing protocol	1× 1% Tween, 3× short rinses in MilliQ	1× 1% Tween, 3× short rinses in MilliQ

hydration and the SC pH gradient. We observed active GCase primarily in the innermost SC layers, which may be related to the slightly acidic pH gradient across the SC. The pH of the inner SC layers (~5–6) is at the optimal pH of GCase [64]. This acidic pH may aid GCase activity in the extracellular SC environment, even at the outermost SC layers that are extremely lipophilic. In relation to Netherton syndrome and atopic dermatitis, changes in environmental factors, like SC humidity and pH gradient, have been reported as possible causes for changes in GCase activity [33, 40, 64- 66]. GCase has been reported as a key mediator for skin barrier homeostasis, as changes in epidermal GCase activity have been observed in cases of skin barrier disruption [67].

In conclusion, we provided two independent methods to visualize epidermal GCase and demonstrated that, in both human skin and our HSEs, active GCase was predominantly present in the extracellular space of the SC lipid matrix. ABP-labeling demonstrated changes in GCase activity for HSEs cultured with inhibitor, explaining the altered SC (glucosyl)ceramide composition in these HSEs. In combination with immunohistochemical staining for the expression of GCase and the use of MS to quantify endogenous GlcCers and ceramides, these methods that visualize active GCase bridge the gap between analysis on protein expression level and the final phenotype, the SC ceramide profile. ABP-labeling is superior to zymography in terms of sensitivity, specificity, and robustness, and the ABP, MDW941, is compatible with skin of human and murine origin [16, 37]. ABP-labeling may therefore be used in future studies to address GCase activity in relation to skin barrier diseases.

Experimental procedures

Processing human skin. Human skin was processed in accordance with the Declaration of Helsinki principles. Skin from mammoplasty or abdominoplasty was obtained from local hospitals directly after surgery. Skin was dermatomed to a thickness of 400 µm after removal of the adipose tissue. Skin samples were either processed to culture HSEs, used for *in vitro* GCase analysis, or cryo-frozen

for sectioning and labeling: small skin samples were put in gelatin capsules filled with matrix specimen Tissue-Tek OCT (Sakura Finetek Europe, Alphen a/d Rijn, The Netherlands) and snap-frozen in liquid nitrogen. Snap-frozen skin tissue from human skin or HSEs was cut to 5 µm-thick sections (Leica CM3050s; Leica Microsystems, Germany). Sections were placed on SuperFrost Plus micro slides (VWR International, The Netherlands) and used for immunohistochemical stainings or enzyme activity studies (*in situ* zymography and ABP-labeling).

Culturing and harvesting HSEs. HSEs were cultured as described previously [34, 68, 69]. Briefly, the epidermis was separated from the dermis by Dispase digestion (Roche, Almere, The Netherlands). Primary fibroblasts were isolated after incubation of the dermis in collagenase (Gibco-Invitrogen, Carlsbad, CA) and Dispase II (Roche). Keratinocytes were isolated from the epidermis after trypsin digestion (Sigma-Aldrich, Steinheim, Germany). The dermal compartment was cultured using isolated rat collagen populated with fibroblasts. Dermal equivalents were cultured submerged for 1 week. Then human keratinocytes were seeded on the dermal equivalent and the HSEs were cultured for 2 days under submerged conditions. The HSEs were lifted to the air-liquid interface and cultured for an additional 2 weeks while supplementing different concentrations of the GCase inhibitor, isofagomine (0, 0.001, 0.01, 0.1, 0.5, 1, 5, or 10 µM; n ≥ 3 for each condition) to the culture medium. Medium was refreshed twice a week. After the culture period, HSEs were harvested: HSEs cultured with 0, 0.5, or 5.0 µM (isofagomine) were snap-frozen (unfixed) and cut in 5 µm-thick sections, as described above for human skin. These samples were analyzed for *in situ* immunohistochemistry-immunofluorescence staining and ABP-labeling of GCase. The remaining HSEs were used to analyze the SC (glucosyl)ceramides by LC/MS.

In vitro *analysis of GCase in human skin lysates.* From dermatomed skin, the individual skin layers were isolated according to the procedures described elsewhere [70, 71]: dermis, epidermis, SC, and viable skin layers (full thickness skin minus SC). Dermis was isolated from the epidermis using a 2.4 U/ml dispase II solution (Roche). SC was isolated by 0.1% trypsin digestion (Sigma-Aldrich). Human skin was left overnight in 0.1% trypsin in PBS at 4°C. After an incubation period of 1 h at 37°C, the SC was isolated and washed once with 0.1% (w/v) trypsin inhibitor in PBS solution and twice in MilliQ. The GCase content was determined in various isolated skin layers for: i) the presence of GCase by Western blotting; ii) the presence of active GCase by ABP-labeling; and iii) quantitation of GCase activity by a 4-MU-β-glc assay. All procedures are described briefly below.

Western blot analysis of GCase. Western blot analysis was performed to examine the presence of GCase in human skin. Skin lysates were prepared in KPI buffer (25 mM potassium phosphate, pH 6.5) and 0.1% (v/v) Triton with cOmplete protease inhibitor (Roche) in tubes with 1.0 mm glass beads (BioSpec Products, Bartlesville, OK). These tubes were processed on a FastPrep-24 5G for 10 cycles of 20 s at a speed of 6 m/s. Samples were filtered on a 1 ml disposable spin column (G-Biosciences, St. Louis, MO) and spun down for 10 min at 15,000 rpm. The protein concentration was quantified by BCA kit (Thermo Scientific, Rockford, IL). Subsequently, lysates were denatured with Laemmli loading buffer [312.5 mM Tris-HCl (pH 6.8), 0.1% (w/v) bromophenol blue, 50% (v/v) glycerol, 10% (w/v) SDS, and 8% (w/v) DTT] and heated for 5 min at 98°C. Samples were subjected to 10% SDS-PAGE and transferred to 0.2 µm nitrocellulose membranes by using a Trans-Blot Turbo system (Bio-Rad). The blots were blocked in 5% (w/v) Protifar in PBS 0.1% (v/v) Tween-20 and incubated overnight at 4°C with anti-GCase monoclonal antibody (8E4 [72]) at 1:1,000 dilution in 2% (w/v) Protifar PBS 0.1% (v/v) Tween-20. After washing three times in PBST, membranes were incubated for 1 h at room temperature with secondary antibody, Alexa Fluor 647 donkey anti-mouse (Life Technologies, Bleiswijk, The Netherlands), at 1:10,000 dilution in 2% (w/v) Protifar PBS 0.1% (v/v) Tween-20. Blots were washed twice in PBST and once in PBS, followed by scanning on a Typhoon FLA 9500 scanner ($\lambda ex = 653$ nm, $\lambda em = 669$ nm). Precision Plus Protein unstained standard #1610373 (Bio-Rad) was used as reference ladder.

ABP-labeling of GCase. To examine whether active GCase was present in lysates of isolated human skin layers, labeling was performed as described previously [16]. Samples were first incubated in 100 nM ABP MDW941 in McIlvaine buffer (150 mM citric acid-Na2HPO4, pH 5.2), 0.2% (w/v) sodium taurocholate, 0.1% (v/v) Triton X-100, and 0.1% (w/v) BSA at 37°C for 1 h. Afterwards, samples were denatured with Laemmli loading buffer and heated for 5 min at 98°C. Gel electrophoresis was performed on 10% SDS-polyacrylamide gels, washed afterwards in demineralized water and visualized using a Typhoon FLA 9500 scanner, deep red ($\lambda ex = 649$ nm, $\lambda em = 670$ nm) and green ($\lambda ex = 532$ nm, $\lambda em = 554$ nm). Bio-Rad #1610373 was used as reference ladder and no significant autofluorescence of the skin layers was observed that could possibly interfere with the results.

GCase activity assay. 4-MU-β-Glc (Santa Cruz, Dallas, TX) was used to measure the GCase activity in the separate skin layers (16). Skin lysates were incubated on ice with and without 100 nM MDW933 (nonfluorescent GCase inhibitor) for 30 min, followed by incubation with the 4-MU-β-Glc mixture at 37°C for 30 min. This incubation mixture contained McIlvaine buffer (150 mM

citric acid-Na_2HPO_4, pH 5.2), 0.2% (w/v) sodium taurocholate, 0.1% (v/v) Triton X-100, 0.1% (w/v) BSA, and 3.7 mM 4-MU-β-Glc substrate. Afterwards, the substrate reaction was stopped with glycine-NaOH (pH 10.3) and the amount of fluorescent product (4-methylumbelliferone) was measured with a fluorescence spectrometer (LS-55; Perkin Elmer) at λex = 366 nm and λem = 445 nm. No significant autofluorescence of the lysates was observed. By subtracting the activity obtained when incubated with GCase inhibitor from the activity obtained without incubation with inhibitor (nonspecific GCase activity), the actual GCase hydrolysis activity was determined.

Immunofluorescence staining for GCase expression. Skin sections (5 μm-thick) were fixed with acetone and washed with PBS (pH 7.4). Sections were blocked using 2.5% (v/v) goat serum in 1% (v/v) BSA/PBS. Incubation with primary monoclonal GCase antibody (ab125065; Abcam, Cambridge, UK) was performed overnight at 4°C. Sections were labeled with secondary antibody (Rhodamine Red AffiniPure goat anti-rabbit IgG; Jackson ImmunoResearch Laboratories, West Grove, PA). Afterwards, sections were washed twice in PBS and once in demineralized water and subsequently mounted using Vectashield with DAPI solution (Vector Laboratories, Burlingame, CA).

In situ *zymography of epidermal GCase.* Skin sections were washed with 1% (v/v) Tween-20 in MilliQ. Afterwards, 1 mM fluorogenic substrate in either 10 mM MES buffer (pH 5.4) or McIlvaine buffer (150 mM citric acid-Na_2HPO_4, pH 5.2) were added to the sections and incubated at 37°C for 0 min, 10 min, 30 min, 1 h, 2 h, or 16 h. Substrate was either 4-MU-β-glc or res-β-glc (Marker Gene Technologies, Oregon). For the zymography competition assay, an additional preincubation step of 1 h at 37°C with 1 mM isofagomine (Toronto Research Chemicals, Toronto, Canada) was performed. Thereafter, the sections were washed briefly with 1% (v/v) Tween-20 solution and subsequently either one or three additional washes with MilliQ water. Sections were mounted with Vectashield containing either DAPI or propidium iodide for appropriate counterstaining of cell nuclei. The main parameters of the optimized protocol are listed in Table 1.

In situ *ABP-labeling of active GCase in the epidermis.* Skin sections were washed with 1% (v/v) Tween-20 (Bio-Rad Laboratories) in MilliQ. Afterwards, different concentrations of the ABP, MDW941 (10, 100, or 1,000 nM), in either McIlvaine buffer or MES buffer were added to the sections and incubated for different periods (0, 10, 30, or 60 min) at 37°C. Negative control samples were preincubated with a 10 μM cyclophellitol-epoxide ABP tagged with a nonfluorescent moiety in 150 mM McIlvaine buffer [150 mM citric acid-Na_2HPO_4 (pH 5.2), 0.2% (w/v) sodium taurocholate, 0.1% (v/v) Triton X-100].

Thereafter, the samples were washed either once or three times in MilliQ water (first wash in addition of 1% Tween-20) and mounted using Vectashield with DAPI solution. An overview of the final method is provided in Table 1.

Fluorescence microscopy. Images were taken using a Zeiss Imager.D2 microscope connected to a Zeiss AxioCam MRm camera (Zeiss, Germany). Images were taken at objective lens magnifications of 20× and 63× (with immersion oil) and with an ocular lens magnification of 10×. Images were processed using Zen 2 2012, blue edition (Zeiss). Exposure times were kept constant for each individual experiment. Gamma was set to 1.0 for all measurements.

SC lipid isolation and (glucosyl)ceramide analysis. SC was isolated from small skin samples by trypsin digestion (as described above). Then, lipids were extracted from the SC using an extended Bligh and Dyer procedure described by Boiten et al. [73] The obtained lipid fraction was reconstituted in heptane:chloroform:methanol (95:21/2:21/2) prior to analysis by LC/MS, as explained previously [73]. In short, chromatography of (glucosyl) ceramides was achieved by an Acquity UPLC H-class (Waters, Milford, MA) using gradient elution of heptane toward 50% heptane:isopropanol:ethanol (50:25:25) by means of a normal phase PVA-silica column (100 × 2.1 mm inner diameter, 5 µm particle size; YMC, Kyoto, Japan). A Xevo TQ-S MS, equipped with an atmospheric pressure chemical ionization source was used for mass analysis in positive-ion full-scan MS mode for scanning from m/z 350 to 1,200 amu (ceramides) and from m/z 500 to 1,350 amu (GlcCers). Deuterated non-hydroxy fatty acid/sphingosine base ceramide (ceramide NS, Evonik Industries, Germany) was used as internal standard. The ratio of the areas under the curve of acyl-GlcCers and acyl-ceramides (specifically ceramide subclasses EOS and EOH, see supplemental Figure S1e, f for the molecular architecture) were subsequently calculated and will be referred to as GlcCer:ceramide ratio, as reported previously [60]. We focused specifically on acyl-ceramide subclasses because: i) the precursors of these ceramides are solely GlcCers and, therefore, only conversion by GCase plays a role in the final step of the acyl-ceramide synthesis and results could not be obscured by other enzymes (i.e., ceramides that can also be generated by acid sphingomyelinase); and ii) these ceramides are crucial for a proper SC lipid matrix structure and are therefore relevant when studying HSEs in relation to the SC barrier.

Acknowledgements

The authors thank Evonik Industries (Essen, Germany) for providing deuterated ceramide NS to quantify LC/MS data.

Supplemental data

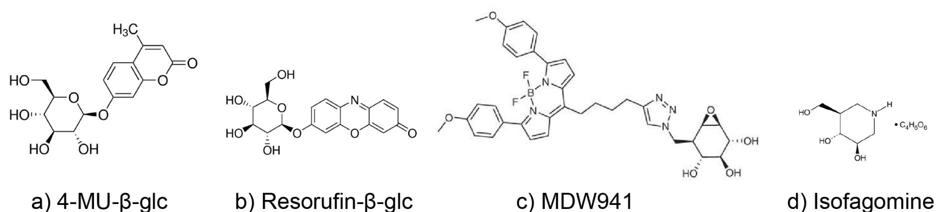

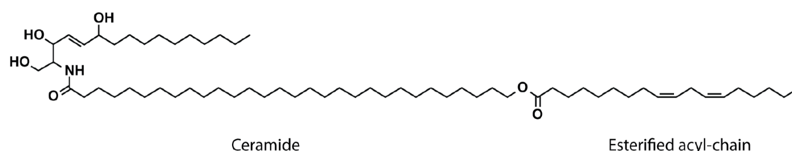

e) Ceramide EOS

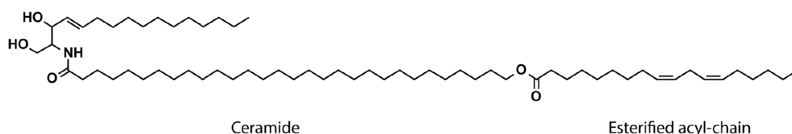

f) Ceramide EOH

Supplemental Figure S1: Molecular structures of a-b) substrates 4-methylumbelliferyl-β-D-glucopyranoside (4-MU-β-glc) and resorufin-β-D-glucopyranoside (Res-β-glc) used for *in situ* zymography that result in respectively blue and red fluorescent products; c) activity-based GCase probe: d) Potent reversible GCase inhibitor. e) Ultra long Esterified Omega-hydroxyacyl-Sphingosine ceramide (Ceramide EOS). f) Ultra long Esterified Omega-hydroxyacyl-6-Hydroxy sphingosine ceramide (Ceramide EOH).

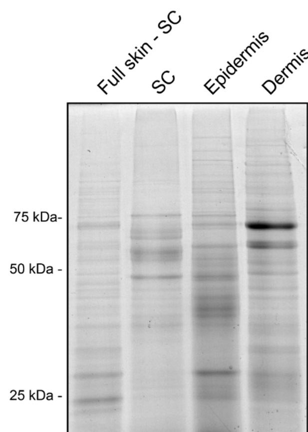

Supplemental Figure S2: Coomassie G250 stain of protein in skin lysate and homogenate. Per lane, 50 μg protein was loaded on the 1.5 mm SDS Page gel.

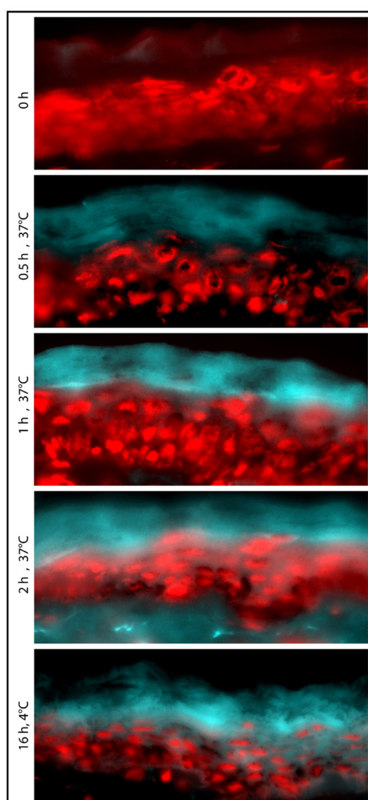

Supplemental Figure S3: Effect of incubation time of zymography assay visualizing GCase activity in human skin sections. 63x magnification images using 4-MU-β-glc substrate focusing on the blue fluorescent product 'layers'. Red counterstaining was performed using propidium iodide to stain cell nuclei. At incubation periods <1 hour, fluorescent signal is relatively low. At incubation periods of 2 hour or longer, diffusion of fluorescent product is observed, particularly after 16 h, when label is 'diffused' at the lower epidermal layers.

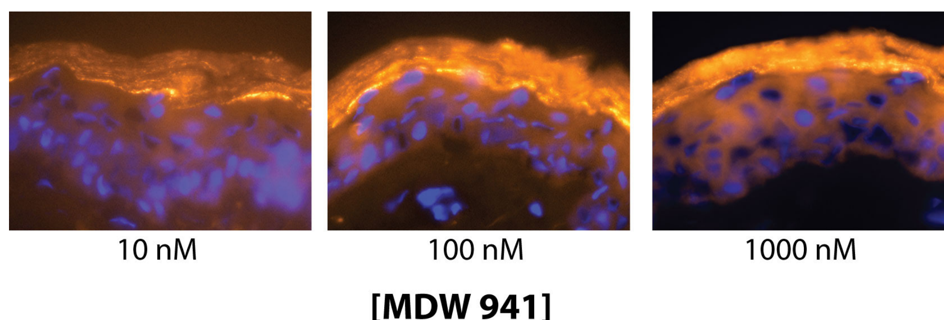

Supplemental Figure S4: *In situ* GCase labeling by MDW941 ABP. 63x Microscope images of human skin sections incubated with different concentrations (10, 100, 1000 nM) of ABP MDW941 (Yellow/Orange), and counterstained with DAPI (blue). GCase labeling was observed for all three MDW941 concentrations, but was optimal around 100 nM.

References

1. W.M. Holleran, Y. Takagi, Y. Uchida, Epidermal sphingolipids: metabolism, function, and roles in skin disorders, FEBS Lett, 580 (2006) 5456–5466.
2. T. Wennekes, R.J. van den Berg, R.G. Boot, G. A. van der Marel, H.S. Overkleeft, J.M. Aerts, Glycosphingolipids–nature, function, and pharmacological modulation, Angew Chem Int Ed Engl, 48 (2009) 8848–8869.
3. B.E. Rosenbloom, N.J. Weinreb, Gaucher disease: a comprehensive review, Crit Rev Oncog, 18 (2013) 163–175.
4. D.L. Stone, W. F. Carey, J. Christodoulou, D. Sillence, P. Nelson, M. Callahan, N. Tayebi, E. Sidransky, Type 2 Gaucher disease: the collodion baby phenotype revisited, Arch Dis Child Fetal Neonatal Ed, 82 (2000) F163–F166.
5. D. Reczek, M. Schwake, J. Schröder, H. Hughes, J. Blanz, X. Jin, W. Brondyk, S. Van Patten, T. Edmunds, P. Saftig, LIMP-2 is a receptor for lysosomal mannose-6-phosphate-independent targeting of beta-glucocerebrosidase, Cell. 131 (2007) 770–783.
6. A.M. Vaccaro, M. Muscillo, K. Suzuki, Characterization of human glucosylsphingosine glucosyl hydrolase and comparison with glucosylceramidase, Eur J Biochem, 146 (1985) 315–321.
7. Y. Takagi, E. Kriehuber, G. Imokawa, P.M. Elias, W.M. Holleran, Beta-glucocerebrosidase activity in mammalian stratum corneum, J Lipid Res, 40 (1999) 861–869.
8. S. van Weely, M. Brandsma, A Strijland, J.M. Tager, J.M. Aerts, Demonstration of the existence of a second, non-lysosomal glucocerebrosidase that is not deficient in Gaucher disease, Biochim Biophys Acta, 1181 (1993) 55–62.
9. M. Horowitz, A. Zimran, Mutations causing Gaucher disease, Hum Mutat, 3 (1994) 1–11.
10. H. Ryšlavá, V. Doubnerová, D. Kavan, O. Vaněk, Effect of posttranslational modifications on enzyme function and assembly, J Proteomics, 92 (2013) 80–109.
11. J. Wilkesman, L. Kurz, Protease analysis by zymography: a review on techniques and patents, Recent Pat Biotechnol, 3 (2009) 175–184.
12. J. Vandooren, N. Geurts, E. Martens, P.E. Van den Steen, G. Opdenakker, Zymography methods for visualizing hydrolytic enzymes. Nat. Methods. 10 (2013) 211–220.
13. S.J. George, J.L. Johnson J. L, In situ zymography, Methods Mol Biol, 622 (2010) 271–277.
14. B.F. Cravatt, A.T. Wright, J.W. Kozarich, Activity-based protein profiling: from enzyme chemistry to proteomic chemistry, Annu Rev Biochem, 77 (2008) 383–414.
15. L.I. Willems, H.S. Overkleeft, S.I. van Kasteren, Current developments in activity-based protein profiling, Bioconjug Chem, 25 (2014) 1181–1191.
16. M.D. Witte, W.W. Kallemeijn, J. Aten J, K.Y. Li, A. Strijland, W.E. Donker-Koopman, A.M. van den Nieuwendijk, B. Bleijlevens, G. Kramer, B.I. Florea, et al, Ultrasensitive in situ visualization of active glucocerebrosidase molecules, Nat Chem Biol, 6 (2010) 907–913.
17. M.D. Witte, G.A. van der Marel, J.M.F.G. Aerts, H.S. Overkleeft, Irreversible inhibitors and activity-based probes as research tools in chemical glycobiology, Org Biomol Chem, 9 (2011) 5908–5926.
18. D. Herrera Moro Chao, W.W. Kallemeijn, A.R. Marques, M. Orre, R. Ottenhoff, C. van Roomen, E. Foppen, M.C. Renner, M. Moeton, M. van Eijk, et al, Visualization of active glucocerebrosidase in rodent brain with high spatial resolution following in situ labeling with fluorescent activity based probes, PLoS One, 10 (2015) e0138107.
19. P.M. Elias, Epidermal lipids, barrier function, and desquamation, J Invest Dermatol 80 (Suppl.) (1983) 44s–49s.
20. K.R. Feingold, P.M. Elias, Role of lipids in the formation and maintenance of the cutaneous permeability barrier, Biochim Biophys Acta, 1841 (2014) 280–294.
21. J. van Smeden, M. Janssens, G.S. Gooris, J.A. Bouwstra. The important role of stratum corneum lipids for the cutaneous barrier function, Biochim Biophys Acta, 1841 (2014) 295–313.
22. J. Ishikawa, H. Narita, N. Kondo, M. Hotta, Y. Takagi, Y. Masukawa, T. Kitahara, Y. Takema, S. Koyano, S. Yamazaki, et al, Changes in the ceramide profile of atopic dermatitis patients, J Invest Dermatol 130 (2010) 2511–2514.
23. Y. Pewzner-Jung, S. Ben-Dor, A.H. Futerman, When do lasses (longevity assurance genes) become CerS (ceramide synthases)? Insights into the regulation of ceramide synthesis, J Biol Chem 281 (2016) 25001–25005.
24. M. Rabionet, K. Gorgas, R. Sandhoff, Ceramide synthesis in the epidermis, Biochim Biophys Acta 1841 (2014) 422–434.
25. M.A. Lampe, M.L. Williams, P.M Elias, Human epidermal lipids: characterization and modulations during

differentiation, J Lipid Res 24 (1983) 131–140.
26. M. Fartasch, The epidermal lamellar body as a multifunctional secretory organelle. In Skin Barrier. P.M. Elias and K.R. Feingold, editors. CRC Press, Boca Raton, FL (2005) 261–272.
27. S. Hamanaka, M. Hara, H. Nishio, F. Otsuka, A. Suzuki, Y. Uchida, Human epidermal glucosylceramides are major precursors of stratum corneum ceramides, J Invest Dermatol, 119 (2002) 416–423.
28. Y.A. Hannun, L.M. Obeid, Principles of bioactive lipid signalling: lessons from sphingolipids, Nat Rev Mol Cell Biol, 9 (2008) 139–150.
29. D. Groen, D.S. Poole, G.S. Gooris, J.A. Bouwstra, Is an orthorhombic lateral packing and a proper lamellar organization important for the skin barrier function? Biochim Biophys Acta 1808 (2011) 1529–1537.
30. J. Bouwstra, G. Gooris, M. Ponec M, The lipid organisation of the skin barrier: liquid and crystalline domains coexist in lamellar phases, J Biol Phys, 28 (2002) 211–223.
31. G.M. Cooper, R.E. Hausman, The Cell: A Molecular Approach. 7th edition Sinauer Associates, Inc, Sunderland, MA (2016)
32. M. Schmuth, K. Schoonjans, Q.C. Yu, J.W. Fluhr, D. Crumrine, J.P. Hachem, P. Lau, J. Auwerx, P.M. Elias, K.R. Feingold, Role of peroxisome proliferator-activated receptor alpha in epidermal development in utero, J Invest Dermatol, 119 (2002) 1298–1303.
33. J.P. Hachem, D. Crumrine, J. Fluhr, B.E. Brown, K.R. Feingold, P.M. Elias, pH directly regulates epidermal permeability barrier homeostasis, and stratum corneum integrity/cohesion, J Invest Dermatol, 121 (2003) 345–353
34. V.S. Thakoersing, G.S. Gooris, A. Mulder, M. Rietveld, A. El Ghalbzouri, J.A. Bouwstra, Unraveling barrier properties of three different in-house human skin equivalents, Tissue Eng Part C Methods, 18 (2012) 1–11.
35. Z. Berger, S. Perkins, C. Ambroise, C. Oborski, M. Calabrese, S. Noell, D. Riddell, W.D. Hirst, Tool compounds robustly increase turnover of an artificial substrate by glucocerebrosidase in human brain lysates, PLoS One, 10 (2015) e0119141.
36. C. Dulsat, N. Mealy, Isofagomine tartrate, Drugs Future, 34 (2009) 23.
37. W.W. Kallemeijn, K.Y. Li, M.D. Witte, A.R. Marques, J. Aten, S. Scheij, J. Jiang, L.I. Willems, T.M. Voorn-Brouwer, C.P. van Roomen, Novel activity-based probes for broad-spectrum profiling of retaining beta-exoglucosidases in situ and in vivo, Angew Chem Int Ed Engl, 51 (2012) 12529–12533.
38. B. Chandrasekar, T. Colby, A. Emran Khan Emon, J. Jiang, T.N. Hong, J.G. Villamor, A. Harzen, H.S. Overkleeft, R.A. van der Hoorn, Broad-range glycosidase activity profiling, Mol Cell Proteomics, 13 (2014) 2787–2800.
39. C. Kuriyama, O. Kamiyama, K. Ikeda, F. Sanae, A. Kato, I. Adachi, T. Imahori, H. Takahata, T. Okamoto, N. Asano, In vitro inhibition of glycogen-degrading enzymes and glycosidases by six-membered sugar mimics and their evaluation in cell cultures, Bioorg Med Chem, 16 (2008) 7330–7336.
40. Y. Hatano, M.Q. Man, Y. Uchida, D. Crumrine, T.C. Scharschmidt, E.G. Kim, T.M. Mauro, K.R. Feingold, P.M. Elias, W.M. Holleran, Maintenance of an acidic stratum corneum prevents emergence of murine atopic dermatitis, J Invest Dermatol, 129 (2009) 1824–1835.
41. D. Ilic, M. Mao-Qiang, D. Crumrine, G. Dolganov, N. Larocque, P. Xu, M. Demerjian, B.E. Brown, S.T. Lim, V. Ossovskaya, et al, Focal adhesion kinase controls pH-dependent epidermal barrier homeostasis by regulating actin-directed Na+/H+ exchanger 1 plasma membrane localization, Am J Pathol, 170 (2007) 2055–2067.
42. J.P. Hachem, T. Roelandt, N. Schurer, X. Pu, J. Fluhr, C. Giddelo, M.Q. Man, D. Crumrine, D. Roseeuw, K.R. Feingold, et al, Acute acidification of stratum corneum membrane domains using polyhydroxyl acids improves lipid processing and inhibits degradation of corneodesmosomes, J Invest Dermatol, 130 (2010) 500–510.
43. Y. Ben-Yoseph, H.L. Nadler, Pitfalls in the use of artificial substrates for the diagnosis of Gaucher's disease, J Clin Pathol, 31 (1978) 1091–1093.
44. F.Y. Choy, R.G. Davidson, Gaucher disease. III. Substrate specificity of glucocerebrosidase and the use of nonlabeled natural substrates for the investigation of patients, Am J Hum Genet, 32 (1980) 670–680.
45. O. Motabar, E. Goldin, W. Leister, K. Liu, N. Southall, W. Huang, J.J. Marugan, E. Sidransky, W. Zheng, A high throughput glucocerebrosidase assay using the natural substrate glucosylceramide, Anal Bioanal Chem, 402 (2012) 731–739.
46. Z.S. Galis, G.K. Sukhova, P. Libby, Microscopic localization of active proteases by in situ zymography: detection of matrix metalloproteinase activity in vascular tissue, FASEB J, 9 (1995) 974–980.
47. S.J. Yan, E.A. Blomme, In situ zymography: a molecular pathology technique to localize endogenous protease activity in tissue sections, Vet Pathol, 40 (2003) 227–236.
48. W.M. Frederiks, O.R. Mook, Metabolic mapping of proteinase activity with emphasis on in situ

zymography of gelatinases: review and protocols, J Histochem Cytochem, 52 (2004) 711–722.
49. R. Patalay, C. Talbot, Y. Alexandrov, I. Munro, M.A.A. Neil, K. Konig, P.M.W French, A. Chu, G.W. Stamp, C. Dunsby, Quantification of cellular autofluorescence of human skin using multiphoton tomography and fluorescence lifetime imaging in two spectral detection channels, Biomed Opt Express, 2 (2011) 3295–3308.
50. K. König, Clinical multiphoton tomography, J Biophotonics, 1 (2008) 13–23.
51. K.D. Collins, Charge density-dependent strength of hydration and biological structure, Biophys J, 72 (1997) 65–76.
52. M.Q. Man, T.K. Lin, J.L. Santiago, A. Celli, L. Zhong, Z.M. Huang, T. Roelandt, M. Hupe, J.P. Sundberg, K.A. Silva, et al, Basis for enhanced barrier function of pigmented skin, J Invest Dermatol, 134 (2014) 2399–2407.
53. R. Nemori, T. Tachikawa, A review for in situ zymography: method for localization of protease activities in a tissue, The Tissue Culture Engineering, 25 (1999) 29–32.
54. S. Fabrega, P. Durand, P. Codogno, C. Bauvy, C. Delomenie, B. Henrissat, B.M. Martin, C. McKinney, E.I. Ginns, J.P. Mornon, et al, Human glucocerebrosidase: heterologous expression of active site mutants in murine null cells, Glycobiology, 10 (2000) 1217–1224.
55. J.M. Aerts, S. Brul, W.E. Donker-Koopman, S. van Weely, G.J. Murray, J.A. Barranger, J.M. Tager, A.W. Schram, Efficient routing of glucocerebrosidase to lysosomes requires complex oligosaccharide chain formation, Biochem Biophys Res Commun, 141 (1986) 452–458.
56. S. Van Weely, J.M. Aerts, M.B. Van Leeuwen, J.C. Heikoop, W.E. Donker-Koopman, J.A. Barranger, J.M. Tager, A.W. Schram, Function of oligosaccharide modification in glucocerebrosidase, a membrane-associated lysosomal hydrolase, Eur J Biochem, 191 (1990) 669–677.
57. F. Ben Bdira, W.W. Kallemeijn, S.V. Oussoren, S. Scheij, B. Bleijlevens, B.I. Florea, C van Roomen, R. Ottenhoff, M. van Kooten, M.T.C. Walvoort, et al, 2017. Stabilization of glucocerebrosidase by active site occupancy, ACS Chem Biol, 12 (2017) 1830–1841.
58. D.J. Urban, W. Zheng, O. Goker-Alpan, A. Jadhav, M.E. Lamarca, J. Inglese, E. Sidransky, C.P. Austin, Optimization and validation of two miniaturized glucocerebrosidase enzyme assays for high throughput screening, Comb Chem High Throughput Screen, 11 (2008) 817–824.
59. Y. Uchida, M. Hara, H. Nishio, E. Sidransky, S. Inoue, F. Otsuka, A. Suzuki, P.M. Elias, W.M. Holleran, S. Hamanaka, Epidermal sphingomyelins are precursors for selected stratum corneum ceramides, J Lipid Res, 41 (2000) 2071–2082.
60. J. van Smeden, M. Janssens, W.A. Boiten, V. van Drongelen, L. Furio, R.J. Vreeken, A. Hovnanian, J.A. Bouwstra, Intercellular skin barrier lipid composition and organization in Netherton syndrome patients, J Invest Dermatol, 134 (2014) 1238–1245.
61. M. Danso, W. Boiten, V. van Drongelen, K. Gmelig Meijling, G. Gooris, A. El Ghalbzouri, S. Absalah, R. Vreeken, S. Kezic, J. van Smeden, et al, Altered expression of epidermal lipid bio-synthesis enzymes in atopic dermatitis skin is accompanied by changes in stratum corneum lipid composition, J Dermatol Sci, 88 (2017) 57–66.
62. A. Sugiura, T. Nomura, A. Mizuno, G. Imokawa, Reevaluation of the non-lesional dry skin in atopic dermatitis by acute barrier disruption: an abnormal permeability barrier homeostasis with defective processing to generate ceramide, Arch Dermatol Res, 306 (2014) 427–440.
63. K. Jin, Y. Higaki, Y. Takagi, K. Higuchi, Y. Yada, M. Kawashima, G. Imokawa, Analysis of beta-glucocerebrosidase and ceramidase activities in atopic and aged dry skin, Acta Derm Venereol, 74 (1994) 337–340.
64. J.W. Fluhr, P.M. Elias, Stratum corneum pH: formation and function of the 'acid mantle', Exogenous Dermatology, 1 (2002) 163–175.
65. M. Abdul-Hammed, B. Breiden, G. Schwarzmann, K. Sandhoff, Lipids regulate the hydrolysis of membrane bound glucosylceramide by lysosomal beta-glucocerebrosidase, J Lipid Res, 58 (2017) 563–577.
66. M.H. Schmid-Wendtner, H. C. Korting, The pH of the skin surface and its impact on the barrier function, Skin Pharmacol Physiol, 19 (2006) 296–302.
67. W.M. Holleran, Y. Takagi, G.K. Menon, S.M. Jackson, J.M. Lee, K.R. Feingold, P.M. Elias, Permeability barrier requirements regulate epidermal beta-glucocerebrosidase, J Lipid Res, 35 (1994) 905–912.
68. A. El Ghalbzouri, S. Commandeur, M.H. Rietveld, A.A. Mulder, R. Willemze, Replacement of animal-derived collagen matrix by human fibroblast-derived dermal matrix for human skin equivalent products, Biomaterials, 30 (2009) 71–78.
69. M. Ponec, A. Weerheim, J. Kempenaar, A. Mulder, G.S. Gooris, J. Bouwstra, A.M. Mommaas, The formation of competent barrier lipids in reconstructed human epidermis requires the presence of vitamin C, J Invest Dermatol, 109 (1997) 348–355.

70. A.K. Nugroho, L. Li, D. Dijkstra, H. Wikstrom, M. Danhof, J.A. Bouwstra, Transdermal iontophoresis of the dopamine agonist 5-OH-DPAT in human skin in vitro, J Control Release, 103 (2005) 393–403.
71. E.M. Haisma, M.H. Rietveld, A. de Breij, J.T. van Dissel, A. El Ghalbzouri, P.H. Nibbering, Inflammatory and antimicrobial responses to methicillin-resistant Staphylococcus aureus in an in vitro wound infection model, PLoS One, 8 (2013) e82800.
72. J.M. Aerts, W.E. Donker-Koopman, G.J. Murray, J.A. Barranger, J.M. Tager, A.W. Schram, A procedure for the rapid purification in high yield of human glucocerebrosidase using immunoaffinity chromatography with monoclonal antibodies, Anal Biochem, 154 (1986) 655–663.
73. W. Boiten, S. Absalah, R. Vreeken, J. Bouwstra, J. van Smeden J, Quantitative analysis of ceramides using a novel lipidomics approach with three dimensional response modelling, Biochim Biophys Acta, 1861 (2016) 1652–1661.